

Gaia: a Window to Large Scale Flows

Adi Nusser¹

Physics Department and the Asher Space Science Institute-Technion, Haifa 32000, Israel

Enzo Branchini²

*Department of Physics, Università Roma Tre, Via della Vasca Navale 84, 00146, Rome, Italy
INFN Sezione di Roma 3, Via della Vasca Navale 84, 00146, Rome, Italy
INAF, Osservatorio Astronomico di Brera, Milano, Italy*

Marc Davis³

Departments of Astronomy & Physics, University of California, Berkeley, CA. 94720

ABSTRACT

Using redshifts as proxy for galaxy distances, estimates of the 2D transverse peculiar velocities of distant galaxies ($cz \lesssim 2 \times 10^4 \text{ km s}^{-1}$) can be obtained from Gaia's measurements of proper motions. Owing to the large number of galaxies expected to be observed by Gaia, these transverse velocities are likely to supersede traditional probes of the large scale velocity field based on current and future distance indicator measurements. This Gaia probe of large scale motions is completely independent of any intrinsic relations between galaxy properties, hence it is essentially free of selection biases. It is also free from homogeneous and inhomogeneous Malmquist biases that typically plague distance indicator catalogs. Further, it provides additional information to traditional probes which yield line-of-sight peculiar velocities.

Subject headings: Cosmology: large scale structure of the Universe, dark matter

1. Introduction

In the standard cosmological paradigm, peculiar motions (i.e. deviations from Hubble flow) of galaxies are the result of the process of gravitational instability with overdense regions attracting material, and underdense regions repelling material. The coherence and amplitude of galaxy flows are a direct indication of the distribution of the dark matter, the cosmological background, and the underlying theory of gravity. Traditionally the peculiar velocity field is derived from observations of distance indicators such as the Tully-Fisher relation (Tully & Fisher 1977) between luminosity

and rotational velocity of galaxies. The observed flux and rotational velocity are then used to infer the distance from the TF relation. The distance is then subtracted from the redshift, cz , in order to obtain the line-of-sight component of the peculiar velocity of a galaxy, with a typical 1σ error $\sim 0.2 \text{ } cz$.

Here we point out an alternative probe of the large scale velocity field. The Gaia (Global Astrometric Interferometer for Astrophysics)¹ space astrometric mission will likely observe $10^6 - 10^7$ galaxies down to $V \sim 20 - 25$ during the period 2013-2018 (e.g. Robin et al. 2012). Gaia will achieve a $\sim 10 \mu\text{as yr}^{-1}$ end-of mission accuracy in measurements of proper motions of objects at $V = 15$. Distances to galaxies are needed to derive

¹E-mail: adi@physics.technion.ac.il

²E-mail: branchin@fis.uniroma3.it

³E-mail: mdavis@berkeley.edu

¹<http://sci.esa.int/science-e/www/area/index.cfm?fareaid=26>

their transverse peculiar velocities (in km s^{-1}) from the proper motions. However, Gaia’s parallax measurements give extremely poor distances for galaxies at 10s of Mpc away from the observer. Therefore, as a proxy for the distance we will use the galaxy’s redshift, cz , which differs from the actual distance by the radial peculiar velocity. The relative error in the transverse velocity as a result of this approximation is small and decreases with redshift. Gaia’s end-of-mission accuracy at $V = 15$, leads to ~ 0.6 cz error in transverse velocities. This is significantly larger than the uncertainty in line-of-sight peculiar velocities from distance indicators. However, we will show that the large number of galaxies expected to be observed with Gaia will beat the increased scatter, possibly making Gaia’s proper motions an excellent probe of the large scale flows. This probe of the large scale flows is completely independent of any assumption on the intrinsic relations of galaxies. Further, the 2D transverse motions are orthogonal (in information content as well as in geometry) to standard line-of-sight peculiar velocities.

The outline of the paper is as follows. In §2 we present the general set up and describe theoretical tools for analyzing future transverse velocity data. We present, in §3, a rough estimate of the expected error in the transverse velocity obtained by smoothing individual velocities. In the concluding section §4, we present a general assessment of the transverse velocity data in comparison to other probes of large scale motions. We also discuss possible sources for redshifts of the population of galaxies expected to be observed by Gaia.

2. Methodology

We will assume an all-sky catalog of redshifts and proper motions. We denote the physical peculiar velocity by \mathbf{v} and the real space comoving coordinate by \mathbf{r} , both expressed in km s^{-1} . Further, $v_{\parallel} = \mathbf{v} \cdot \hat{\mathbf{r}}$ and $\mathbf{v}_{\perp} = \mathbf{v} - v_{\parallel} \hat{\mathbf{r}}$ are, respectively, the components of \mathbf{v} parallel and perpendicular to the line-of-sight, where $\hat{\mathbf{r}}$ is a unit vector in the line-of-sight direction. We restrict the analysis to $cz \lesssim 15000 \text{ km s}^{-1}$ and neglect cosmological geometric effects, so that the redshift coordinate is $\mathbf{s} = \mathbf{r} + v_{\parallel} \hat{\mathbf{r}}$. Note $\hat{\mathbf{s}} = \hat{\mathbf{r}}$ and $cz = r + v_{\parallel} = \mathbf{s} \cdot \hat{\mathbf{r}} = s$.

Proper motions transverse to the line-of-sight will be denoted by $\boldsymbol{\mu}$. The transverse 2D space velocity is of a galaxy at real space distance r is

$$\begin{aligned} \mathbf{v}_{\perp} &= r \boldsymbol{\mu} \\ &= 677.22 \frac{\boldsymbol{\mu}}{1 \mu\text{as yr}^{-1}} \frac{r}{10^4 \text{ km s}^{-1}} \frac{70 \text{ km s}^{-1} \text{Mpc}^{-1}}{H_0}, \end{aligned} \quad (1)$$

which corresponds a transverse peculiar velocity of 474 km s^{-1} for $1 \mu\text{as yr}^{-1}$ at $d = 100 \text{ Mpc}$. Hereafter we use $H_0 = 70 \text{ km s}^{-1} \text{Mpc}^{-1}$ to set the distance scale.

However, the distances, r , are unknown, and, therefore, we make the approximation

$$\mathbf{v}_{\perp} = s \boldsymbol{\mu}. \quad (2)$$

This introduces a relative error v_{\parallel}/cz in the determination of \mathbf{v}_{\perp} where $\langle v_{\parallel}^2 \rangle^{1/2} \sim 200 - 300 \text{ km s}^{-1}$ (?). Hence the error is negligible as we go to $cz \gtrsim 2000 \text{ km s}^{-1}$. The error is also random since $\langle \mathbf{v}_{\perp} v_{\parallel} \rangle = 0$.

Therefore, the estimated velocity field will be given as a function of the redshift space coordinate. To linear order, velocity fields expressed in real and redshift spaces are equivalent. In the quasilinear regime, dynamical relations can be derived for the velocity field in redshift space (Nusser & Davis 1995), thanks to the interesting property that an irrotational (or potential) flow in real space remain irrotational also in redshift space (Chodorowski & Nusser 1999).

2.1. From 2D transverse velocities to 3D flows

Here we offer basic expressions for the derivation of the full peculiar velocity field $\mathbf{v}(\mathbf{s})$ from the smoothed 2D transverse velocity field, $\mathbf{v}_{\perp}(\mathbf{s})$. Assuming a potential flow $\mathbf{v}(\mathbf{s}) = -\nabla \Phi(\mathbf{s})$ and expanding the angular dependence of Φ in spherical harmonics, $\Phi(\mathbf{s}) = \sum_{lm} \Phi_{lm}(s) Y_{lm}(\hat{\mathbf{s}})$, gives (Arfken & Weber 2005)

$$v_{\parallel} = - \sum_{lm} \frac{d\Phi_{lm}}{ds} Y_{lm} \quad (3)$$

$$\mathbf{v}_{\perp} = - \sum_{lm} \frac{\Phi_{lm}}{s} \boldsymbol{\Psi}_{lm}, \quad (4)$$

where $\boldsymbol{\Psi}_{lm} = r \nabla Y_{lm}$ is the vector spherical harmonic. Thanks to the orthogonality conditions

$\int d\Omega \Psi_{lm} \cdot \Psi_{l'm'} = l(l+1) \delta_{ll'}^K \delta_{mm'}^K$, the potential coefficients can be recovered by

$$\Phi_{lm}(s) = \frac{-1}{l(l+1)} \int d\Omega \mathbf{v}_\perp(\mathbf{s}) \cdot \Psi_{lm}(\hat{\mathbf{s}}), \quad (5)$$

for $l > 0$. This means that $\Phi(\mathbf{s})$ can be recovered from the \mathbf{v}_\perp up-to a monopole term which corresponds to a purely radial flow with zero transverse motions. That is not a serious drawback since the monopole term can always be removed from the predictions of any model to be compared with the data.

2.2. Testing the potential flow anzats

Initial conditions in the early Universe might have been somewhat chaotic, so that the original peculiar velocity field was uncorrelated with the mass distribution, or even contained vorticity (e.g. Christopherson et al. 2011). At late time, a cosmological velocity field should have a negligible rotational component, \mathbf{v}^{rot} on large scale, away from orbit mixing regions. The reason is that any circulation, $\Gamma = \oint \mathbf{v}^{\text{rot}} \cdot d\mathbf{s}$, is conserved by Kelvin's theorem. Hence, any rotational component will be decaying as $1/a$, where a is the scale factor. In contrast, the irrotational component of the peculiar velocity will have a growing $v \sim \sqrt{a}$. Therefore, on large scales, away from collapsed objects, the irrotational component is expected to be negligible. The absence of any significant large scale vorticity is, therefore, a strong prediction of the standard cosmological paradigm. To assess this prediction, the observed transverse motions can be used to constrain the amplitude of the irrotational component. This can be done by writing the transverse component of \mathbf{v}^{rot} as (Arfken & Weber 2005)

$$\mathbf{v}_\perp^{\text{rot}} = \sum_{lm} V_{lm}^{\text{rot}} \Phi_{lm}, \quad (6)$$

where $\Phi_{lm} = \mathbf{s} \times \nabla Y_{lm}$ belong to another class of vector spherical harmonics that satisfy the same orthogonality conditions as Ψ . Hence, V_{lm}^{rot} is equal to the r.h.s of Eq. 5 but with Φ_{lm} instead of Ψ_{lm} . Further, $\int d\Omega \Phi_{lm} \cdot \Psi_{l'm'} = 0$, hence the recovery of the rotational mode is formally independent of the potential flow mode.

3. The expected errors

We provide estimates of the expected random errors in the smoothed transverse velocity field, $\mathbf{v}_\perp(\mathbf{s})$, as a function of distance from the observer z .

The expected 1σ error, σ_μ , in the measurement of an object's proper motion depends on its G magnitude and, to a lesser extent, on its color (de Bruijne 2012). Jordi et al. (2010) give relations between Gaia's $G(350 - 1000 \text{ nm})$ magnitude and the more familiar V and I_c . Using these relations we find $G \approx V - 0.27$, which is obtained with $V - I_c \approx 1$ as is appropriate for galaxies (Fukugita et al. 1995). Hereafter, we will use σ_μ as a function of G , according to the expression referenced in de Bruijne (2012) assuming a constant $V - I_c = 1$ for all galaxies. This σ_μ is plotted in left panel of Fig. 1. Another useful quantity is the average galaxy measurement error as a function of redshift, cz , i.e. $\int^{m_{lim}} dm n(m, cz) \sigma_\mu(m) / \int^{m_{lim}} dm n(m, cz)$ where $n(m, cz)$ is the number density of galaxies (at redshift $cz = s$) per unit volume and per magnitude m and m_{lim} is the magnitude cut. Given the luminosity function $N(M)$ we have $n(m, cz) dm = N(M) dM$ where $M = m - 5 \log_{10}(cz) - 15$ is the absolute magnitude. For Gaia's G band, we approximate $N(M)$ by the Schechter form of the V band luminosity function taking into account that $G - V = -0.26$ as explained above. Here we adopt the Schechter parameters given by (Brown et al. 2001). Other choices for the Schechter parameters of the V luminosity function (Marchesini et al. 2012) do not change the results significantly at the magnitude limits considered here. The results for the average error are shown in the right panel for three magnitude cuts. The flatness of the curves for all magnitude, is a reflection of the fact that number of galaxies increases strongly with magnitude.

Given individual measurements $\mathbf{v}_{\perp i} = \mathbf{v}_\perp(\mathbf{s}_i)$

² In generating the smoothed $\mathbf{v}_\perp(\mathbf{s})$ care must be employed since the transverse directions of galaxies in different sight-lines within a filtering window do not point in the same direction. This difficulty could be overcome by tensor window smoothing à la POTENT (Dekel et al. 1990). However, we will not be concerned with these fine details at this stage.

write the smoothed velocity as

$$\mathbf{v}_\perp(\mathbf{s}) = \frac{\sum_i \mathbf{v}_{\perp i} \sigma_{\perp i}^{-2} W(\mathbf{s}, \mathbf{s}_i)}{\sum_i \sigma_{\perp i}^{-2} W(\mathbf{s}, \mathbf{s}_i)} \quad (7)$$

where the summation is over all galaxies, $\sigma_{\perp i} = s\sigma_{\mu i}$ and W is a smoothing window function.

The 1σ errors on $\mathbf{v}_\perp(\mathbf{s})$ is given by

$$\sigma_\perp^2(\mathbf{s}) = \frac{\sum_i \sigma_{\perp i}^{-2} W^2(\mathbf{s}, \mathbf{s}_i)}{[\sum_i \sigma_{\perp i}^{-2} W(\mathbf{s}, \mathbf{s}_i)]^2}. \quad (8)$$

The summation over galaxies can be transformed into a volume integration with the same argument but multiplied by the number density of galaxies. Doing so for a uniform distribution and assuming a Gaussian window, W , of width R_G , we get

$$\sigma_\perp^2(s) = \frac{s^2}{8\pi^{3/2} R_G^3} \frac{1}{\int^{m_{lim}} dm n(m, cz) \sigma_\mu^{-2}(m)}, \quad (9)$$

we have assumed the distant observer limit so that $|\mathbf{s}_i - \mathbf{s}| \ll s$. For a Top-Hat window of the same width we get the same expression but with $4\pi/3$ as the numerical factor in the denominator. Substituting $\sigma_\mu(m)$ (see left panel Fig. 1) in Eq. 9, we compute the expected error, σ_\perp , in the smoothed \mathbf{v}_\perp , for a gaussian smoothing with $R_G = 1500 \text{ km s}^{-1}$. The top panel in Fig. 2 shows curves of σ_\perp as a function of distance for three magnitude cuts. For comparison the figure also plots the error in the filtered line-of-sight peculiar velocities in the SFI++ catalog of TF measurements of ~ 4000 galaxies (Masters et al. 2006). There is a significance decrease in σ_\perp as the magnitude is increased from $G = 14$ to 15, but the improvement is not as dramatic when fainter galaxies with $15 < G < 16$ are included. The reason is the rapid deterioration in σ_μ at $G = 16$ which is not compensated by the added number of fainter galaxies. At redshifts $cz \gtrsim 6000 \text{ km s}^{-1}$ and for $G < 15$, peculiar velocities from Gaia's proper motions are expected to fair much better than the SFI++ catalog. Another important quantity which can be computed from transverse velocities is the dipole motion (i.e. bulk flow) of spherical shells of a given thickness. This motion is described by a constant term \mathbf{B} and gives rise to a transverse velocity field of the form $\mathbf{v}_{\perp B} = \mathbf{B} - \hat{\mathbf{r}}(\mathbf{B} \cdot \hat{\mathbf{r}})$. The dipole term \mathbf{B} can be found by least squares fitting of $\mathbf{v}_{\perp B}$ to the observed velocities $\mathbf{v}_{\perp i}$. The expected error in

\mathbf{B} as a function of distance of the shell, is plotted in the bottom panel in Fig. 2. Predictions for 3 magnitude cuts are plotted for spherical shells of 3000 km s^{-1} in thickness. For comparison we also plot the WMAP7 Λ CDM model (Larson et al. 2010) predictions for the amplitude of the velocity dipole on spherical shells. It is encouraging that the predicted amplitude is larger than the expected error out to relatively large distances.

4. Discussion

The number of galaxies expected to be observed by Gaia is likely to exceed standard distance indicator data by two orders of magnitude (Masters et al. 2006; Springob et al. 2012; Masters et al. 2008; Courtois et al. 2011). Despite the larger object-by-object error, this makes the method presented here a serious contender to traditional probes of the peculiar velocity field. The method has several advantages. Firstly, it is completely independent of any assumed intrinsic relations of galaxies and, hence, it does not suffer from the usual concerns related to these relations, e.g. linearity, selection biases and dependence on environment. Secondly, it yields the 2D transverse velocity component and hence it offers completely orthogonal information to standard probes which yield the line-sight-component. Thirdly, it is free from homogeneous and inhomogeneous Malmquist biases (Lynden-Bell et al. 1988).

The usefulness of the method for probing the 3D velocity field on scales of a few 10s of Mpc is limited to $cz \lesssim 10^4 \text{ km s}^{-1}$. However, large scale moments of the velocity field can be assessed at much larger distances. In particular the error of the dipole on (i.e. bulk flow of) spherical shells can be estimated with $\sim 100 - 200 \text{ km s}^{-1}$ error at $cz \sim 1.5 \times 10^4 \text{ km s}^{-1}$. At larger redshifts, neither this method nor traditional ones are comparable to the constraints on the dipole from galaxy luminosities in future galaxy redshift surveys (Nusser et al. 2011). At lower distances ($< 2000 \text{ km s}^{-1}$) the the transverse motions of galaxies could play an important role at providing new constraints on the motion of Local Group of galaxies.

Gaia will provide spectroscopic information of unresolved galaxies (?). But the inferred redshifts may not be sufficiently accurate for all unresolved galaxies with astrometric data (e.g. Robin et al.

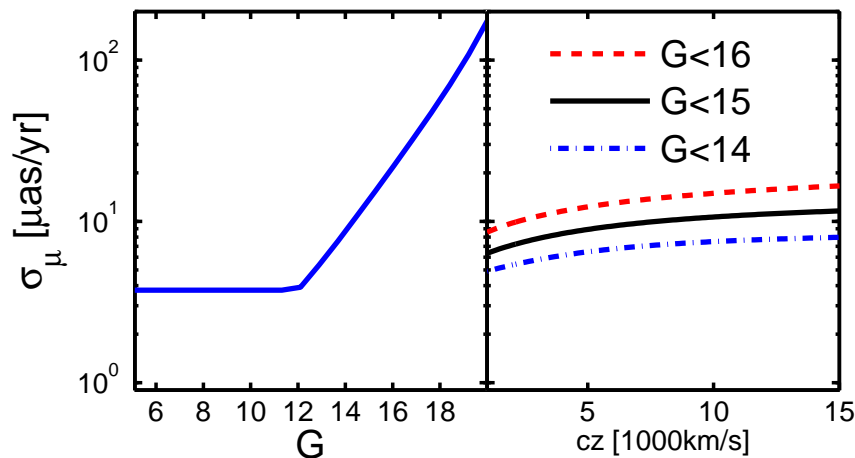


Fig. 1.— Expected error in Gaia’s proper motion measurements. *Left*: 1σ error of an object as a function of its G magnitude. *Right*: mean 1σ error of objects as a function of distant for three values of the G magnitude cut.

2012). The Two Mass Redshift Survey (2MRS; Huchra et al. 2011) offers redshifts of $\sim 4 \times 10^4$ galaxies down to $K_s = 11.75$. This is the deepest all-sky redshift catalog currently available. It was originally planned to reach up to $K=12.2$ mag and to include $\sim 10^5$ galaxies. Using $G \approx V - 0.27$ and the observed V band luminosity function (Brown et al. 2001), the expected number of galaxies brighter than $V = 15.27$ (i.e. $G = 15$) is $\sim 10^5$, similar to the expected number for $K_s = 12.2$. Further, $K_s \approx K$ (Carpenter 2001) and $V - K > 2.7$ for most galaxies (Aaronson 1978), we conclude that the $K_s = 12.2$ 2MRS redshifts would correspond to most of Gaia galaxies observed to $G = 15$. This is particularly interesting as Gaia’s astrometric accuracy deteriorate rapidly at fainter objects. However, it is unclear if 2MRS will be continued to $K_s = 12.2$ in the very near future (Macri, private communication). For the purpose of the analysis presented here one could use a catalog of photometric redshifts based on the 2MASS galaxy catalog (Skrutskie et al. 2006), containing almost 1 million sources with $K_s < 13.5$ mag. Its current form (2MASS XSCz, Jarrett 2004) offers errors as large as 20-25%, which will improve in the coming years using the data from other galaxy catalogs for the photo- z estimation (Bilicki, private communication).

We have restricted the error analysis here to $G \sim 15$ since redshifts will probably not be available for all fainter galaxies. However, data at fainter magnitudes can well be exploited by computing the dipole as a function of an effective depth corresponding to a certain magnitude range. This can then be compared with model predictions for an equivalent quantity (Bilicki et al. 2011).

5. Acknowledgments

We thank Maciej Bilicki for useful comments. This work was supported by THE ISRAEL SCIENCE FOUNDATION (grant No.203/09), the German-Israeli Foundation for Research and Development and the Asher Space Research Institute. MD acknowledges the support provided by the NSF grant AST-0807630. EB acknowledges the support provided by the Agenzia Spaziale Italiana (ASI, contract N.I/058/08/0) EB thanks the Technion Physics Department for the kind hospitality. AN is grateful for the hospitality of the Physics Department, Università Roma Tre. EB thanks Michele Bellazzini for suggestions and discussions.

REFERENCES

Aaronson, M. 1978, ApJL, 221, L103

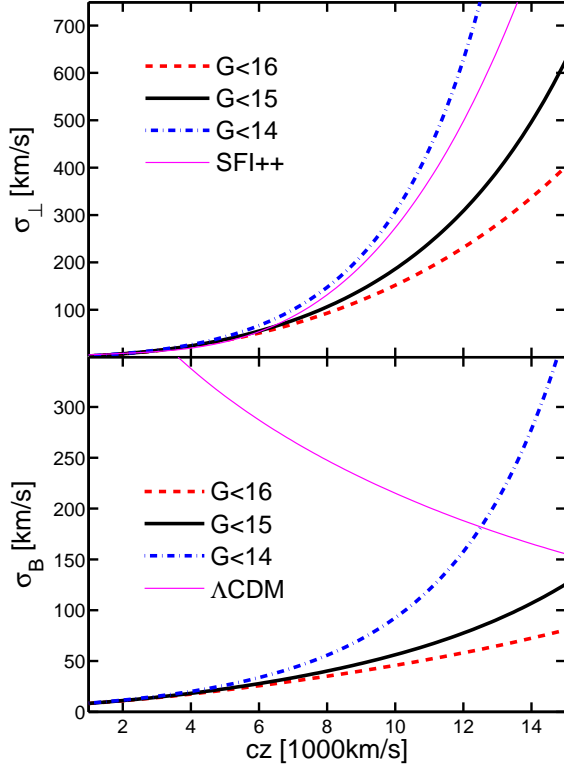


Fig. 2.— Expected errors (1σ) on two quantities computed from the Gaia astrometric galaxy data. *Top*: Errors in the 2D transverse peculiar velocity field obtained by filtering the data with a gaussian window of width $R_G = 1500 \text{ km s}^{-1}$. For comparison, the thin solid magenta line is the error in the SFI++ line-of-sight peculiar velocities smoothed with the same window. Errors scale like $R_G^{3/2}$. *Bottom*: Errors in the bulk (dipole) motion of spherical shells of thickness $\Delta cz = 3000 \text{ km s}^{-1}$. Errors scale like $(\Delta cz)^{1/2}$. For reference, predictions from the WMAP7 Λ CDM for the dipole on shells are also plotted. In both panels, dash-dotted, solid and dotted curves correspond to $G=14$, 15 & 16 magnitude cuts, as indicated in the figure.

- Arfken, G. B., & Weber, H. J. 2005, *Mathematical methods for physicists* 6th ed. (Elsevier)
- Bilicki, M., Chodorowski, M., Jarrett, T., & Mamon, G. A. 2011, *ApJ*, 741, 31
- Brown, W. R., Geller, M. J., Fabricant, D. G., & Kurtz, M. J. 2001, *AJ*, 122, 714
- Carpenter, J. M. 2001, *AJ*, 121, 2851
- Chodorowski, M. J., & Nusser, A. 1999, *MNRAS*, 309, L30
- Christopherson, A. J., Malik, K. A., & Matraavers, D. R. 2011, *Physical Review D*, 83, 123512
- Courtois, H. M., Tully, R. B., & Héraudeau, P. 2011, *MNRAS*, 415, 1935
- de Bruijne, J. H. J. 2012, *ArXiv*1201.3238
- Dekel, A., Bertschinger, E., & Faber, S. M. 1990, *ApJ*, 364, 349
- Fukugita, M., Shimasaku, K., & Ichikawa, T. 1995, *PASP*, 107, 945
- Huchra, J. P., Macri, L. M., Masters, K. L., Jarrett, T. H., Berlind, P., Calkins, M., Crook, A. C., Cutri, R., Erdogan, P., Falco, E., George, T., Hutcheson, C. M., Lahav, O., Mader, J., Mink, J. D., Martimbeau, N., Schneider, S., Skrutskie, M., Tokarz, S., & Westover, M. 2011, *ArXiv*:1108.0669
- Jordi, C., Gebran, M., Carrasco, J. M., de Bruijne, J., Voss, H., Fabricius, C., Knude, J., Vallenari, A., Kohley, R., & Mora, A. 2010, *A&A*, 523, A48
- Larson, D., Dunkley, J., Hinshaw, G., Komatsu, E., Nolte, M. R., Bennett, C. L., Gold, B., Halpern, M., & Hill, e. a. 2010, *ArXiv e-prints*
- Lynden-Bell, D., Faber, S. M., Burstein, D., Davies, R. L., Dressler, A., Terlevich, R. J., & Wegner, G. 1988, *ApJ*, 326, 19
- Marchesini, D., Stefanon, M., Brammer, G. B., & Whitaker, K. E. 2012, *ArXiv e-prints*
- Masters, K. L., Springob, C. M., Haynes, M. P., & Giovanelli, R. 2006, *ApJ*, 653, 861
- Masters, K. L., Springob, C. M., & Huchra, J. P. 2008, *AJ*, 135, 1738

- Nusser, A., Branchini, E., & Davis, M. 2011, *ApJ*, 735, 77
- Nusser, A., & Davis, M. 1995, *MNRAS*, 276, 1391
- Robin, A. C., Luri, X., Reyl  , C., Isasi, Y., Grux, E., Blanco-Cuaresma, S., Arenou, F., Babusiaux, C., Belcheva, M., Drimmel, R., Jordi, C., Krone-Martins, A., Masana, E., Mauduit, J. C., Mignard, F., Mowlavi, N., Rocca-Volmerange, B., Sartoretti, P., Slezak, E., & Sozzetti, A. 2012, *ArXiv1202.0132*
- Springob, C. M., Magoulas, C., Proctor, R., Colless, M., Jones, D. H., Kobayashi, C., Campbell, L., Lucey, J., & Mould, J. 2012, *MNRAS*, 2337
- Tully, R. B., & Fisher, J. R. 1977, *A&A*, 54, 661